

Yb Fiber Laser Pumped Mid-IR Source Based on Difference Frequency Generation and Its Application to Ammonia Detection

Naoya MATSUOKA, Shigeru YAMAGUCHI, Kenzo NANRI, Tomoo FUJIOKA,
Dirk RICHTER¹ and Frank K. TITTEL¹

Department of Physics, School of Science, Tokai University, Kanagawa 259-1292, Japan

¹Rice Quantum Institute, Rice University, Houston, TX 77251-1892, USA

(Received October 10, 2000; accepted for publication October 30, 2000)

A Yb fiber laser pumped cw narrow-linewidth tunable mid-IR source based on a difference frequency generation (DFG) in a periodically poled LiNbO₃ (PPLN) crystal for trace gas detection was demonstrated. A high power Yb fiber laser and a distributed feedback (DFB) laser diode were used as DFG pump sources. This source generates mid-IR at 3 μm with a power of ~2.5 μW and a spectral linewidth of less than 30 MHz. A frequency tuning range of 300 GHz (10 cm⁻¹) was obtained by varying the current and temperature of the DFB laser diode. A high-resolution NH₃ absorption Doppler-broadened spectrum at 3295.4 cm⁻¹ (3.0345 μm) was obtained at a cell pressure of 27 Pa from which a detection sensitivity of 24 ppm·m was estimated.

KEYWORDS: difference frequency generation, cw mid infrared source, Yb fiber laser, PPLN crystal, NH₃ detection, laser spectroscopy

1. Introduction

Tunable cw narrow linewidth mid-IR sources are useful spectroscopic tools for trace gas detection since numerous gas species exhibit fundamental ro-vibrational absorption lines with high absorption strengths in the mid-IR spectral region such as ammonia (3.0 μm), methane (3.3 μm), formaldehyde (3.5 μm), and carbon dioxide (4.3 μm). The spectroscopic source reported in this paper is based on the difference frequency generation (DFG)^{1–6} where two near-IR laser pump sources (λ_1, λ_2) are frequency-mixed to generate mid-IR ($\lambda_3 = (1/\lambda_1 - 1/\lambda_2)^{-1}$) in a bulk quasi-phase-matched (QPM) periodically poled LiNbO₃ (PPLN) crystal⁷ in a single-pass geometry. The DFG spectroscopic source operates at room temperature with single spatial mode, single frequency and continuously tunable over a wide frequency region.^{2,3,6} Compact DFG-source based gas sensors capable of sensitive real-time gas detection have been demonstrated for field use.^{8–10} Furthermore, such sources offer an intrinsic spectral resolution of less than 0.001 cm⁻¹ (30 MHz) without active frequency stabilization, which is better than a typical FTIR (Fourier Transform Infrared) spectrometer with of ~0.1 cm⁻¹ (3 GHz) resolution.

Other cw mid-IR coherent sources include lead salt, anti-mony based diode lasers¹¹ and more recently quantum cascade lasers,¹² but all require cryogenic cooling. Cw optical parametric oscillators (OPO)¹³ have been demonstrated, but they require improvements in effective single frequency control and scanning. To enhance the DFG conversion efficiency in PPLN, a waveguide structure has been implemented in PPLN by other groups (Hofmann *et al.*,¹⁴) (Petrov *et al.*)¹⁵ but at a cost of DFG pumping complexity.

The mid-IR wavelength range by DFG is determined by the commercial availability of single frequency cw high power laser pump sources and the transparency range of the nonlinear optical material. Novel nonlinear QPM materials have been applied such as LiNbO₃ (transparency range: 0.4–5 μm) by Fejer *et al.*,⁷ MgO-doped LiNbO₃ by Saito *et al.*¹⁶ and RbKTiOAsO₄ by Frandkin-Kashi *et al.*¹⁷ For a pump source, various solid state and diode lasers have been used

to date^{1–6} including external cavity diode laser (ECDL) by Goldberg. *et al.*²) and Cr₃:LiSrAlF₆ laser by Parhat *et al.*¹⁸ Recently, compact tunable telecommunications DFB laser diodes have become commercially available in a standardized ITU (International Telecommunication Union) 50 GHz spaced frequency grid in a range of 1492–1530 nm (S band), 1530–1570 nm (C band) and 1570–1612 nm (L band).

In this work, we utilize a compact Yb fiber laser as one of the pump sources for DFG in a PPLN crystal. The fiber laser can be designed to operate at any specified wavelength within the range from 1035 to 1120 nm corresponding to Yb doped fiber amplifier gain region.^{19,20} Hence the mid-IR range from 2.9 μm to 4.5 μm becomes readily accessible by selecting a Yb pump wavelength together with the appropriate ITU telecommunications DFB laser diode. For the generation of ~3 μm in PPLN, we use a 1038 nm Yb fiber laser and a 1577 nm telecommunication DFB laser diode as effective DFG pump sources. To improve the ruggedness of the DFG source for field application, the use of fiber delivery from pump source to the crystal was introduced by Petrov *et al.*²¹ The fiber and diode lasers used in this work are fiber-coupled (without any free space optics), combined by a fiber wavelength division multi-plexer (WDM) and imaged into the PPLN crystal with a microscope lens. Such an all-fiber-based DFG pump architecture realizes a permanently aligned and robust optical module.

This DFG source is applied to NH₃ detection which is of interest in various applications such as in combustion, in chemical analysis and in environmental trace gas monitoring. The spectral characteristics of DFG output, such as linewidth and tunability are evaluated from a Doppler-broadened NH₃ spectrum obtained at a reduced-pressure. The detection limit of NH₃ concentration is inferred from the experiment for future gas sensor development. To the best of our knowledge, this work reports the first demonstration of a fiber laser pumped DFG based mid-IR source for trace gas sensing, and the first detection of NH₃ line at ~3 μm with a high-resolution DFG based spectroscopic source using a PPLN crystal.

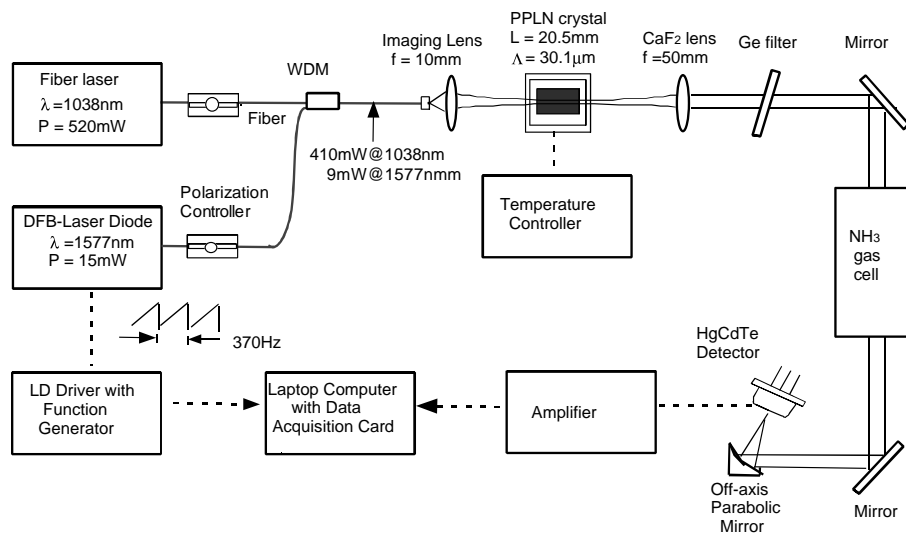


Fig. 1. Schematic of a mid-IR $3\ \mu\text{m}$ spectroscopic DFG source configured for NH_3 gas detection.

2. Experimental Details

The schematic of the mid-IR $3\ \mu\text{m}$ DFG spectroscopic source and trace NH_3 gas detection system is shown in Fig. 1. One of the DFG pump sources is a frequency-fixed Yb fiber laser, consisting of two stages: a fiber grating controlled seed laser oscillator and a double cladding Yb fiber amplifier stage. The fiber laser operates at 1038 nm with an output power of 520 mW and a linewidth of <1 MHz. The other DFG pump source is a frequency-tunable 1577 nm DFB laser diode (LD) with an output power of 15 mW and a linewidth of 1 MHz. The LD frequency can be varied by $\sim 0.02\ \text{cm}^{-1}/\text{mA}$ with current and $\sim 0.35\ \text{cm}^{-1}/\text{K}$ with temperature. Both pump sources are fiber-coupled and these beams are combined by WDM. The fiber connection between laser sources and the WDM causes a power loss due to a WDM insertion loss (<0.5 dB) and a loss associated with mis-match in the mode field diameter of each fiber. The multiplexed beams are emitted to free space from the APC (angled polished coupler) fiber end. The emitted beams have a Gaussian spatial profile and are focused to a diameter of about $80\ \mu\text{m}$ into the center of the PPLN crystal by an imaging (microscope objective) lens ($f = 10$ mm). Polarization controllers are inserted after each pumping source to match the nonlinear optical polarization state of each source to be linearly and vertically polarized to optimize the nonlinear interaction of the “ $e + e \rightarrow e$ ” DFG mixing process in the PPLN crystal.²²⁾

The PPLN crystal used in this experiment is 20.5 mm long, 0.5 mm thick and with 10 channels of grating period ranging from $29.60\ \mu\text{m}$ to $30.50\ \mu\text{m}$ in increments of $0.1\ \mu\text{m}$ and 0.88 mm wide for each channel, which provides flexibility to phase-match with the available wavelength selection of pump laser sources. The PPLN crystal temperature is controlled by placing it on a Peltier thermo-electric element. The phase-match condition, $n_3/\lambda_3 = n_1/\lambda_1 - n_2/\lambda_2 - \Lambda$ (where Λ is the grating period and n_i ($i = 1-3$) is the extraordinary refractive index calculated from Sellmeier's equation²³⁾), is achieved with the $30.10\ \mu\text{m}$ PPLN grating period at 26°C . Both surfaces of the PPLN crystal are anti-reflection-coated for the two pump wavelengths (pump and signal: $<0.5\%$) and output wavelength (idler: 3.5%). The phase matching band-

width is $\sim 20\ \text{cm}^{-1}$ (600 GHz).²²⁾ The generated mid-IR DFG radiation is collimated by a CaF_2 lens ($f = 50$ mm). The unconverted residual pump-beams are blocked by a Ge filter.

NH_3 gas detection was performed in order to evaluate the performance of the DFG spectroscopic source by using a 10.2 cm-long absorption glass cell fitted with CaF_2 windows. The frequency of the DFG spectroscopic source can be scanned $0.6\ \text{cm}^{-1}$ by applying current modulation of 40 mA at a ~ 370 Hz scan-rate to the DFB LD, provided by a function generator which is a part of the LD driver. For wide-range DFG frequency tuning, the DFB LD temperature is varied from 5°C to 35°C in $\sim 1^\circ\text{C}$ increments (corresponding to a $0.35\ \text{cm}^{-1}$ increments). The DFG probe beam exiting from the gas cell is collected by an off-axis parabolic mirror ($f = 50$ mm) and focused onto a thermoelectrically cooled HgCdTe detector with $1\ \text{mm}^2$ active area. The detected signal is amplified and acquired by laptop computer with a 16 bit A/D data acquisition card. The sampling frequency is set at 200 kHz and the signal data is averaged over 500 sweeps. The signal data is analyzed using LabVIEW software (National Instrument). A beam stop is placed after the Ge filter to block the beam to determine a reference dark voltage. An absorption spectrum is obtained by subtracting the reference data from the signal data and applying a third order polynomial fit to the detector baseline.

3. Experimental Results and Discussion

In a preliminary experiment, the polarization characteristics of the fiber laser are investigated (see Fig. 2) in order to determine whether any polarization effects might lead to power fluctuations of DFG spectroscopic source. For this investigation, a polarizer (Nicol prism) is placed between the fiber laser and a Ge detector. After adjusting the polarization to be linear using one of the polarization controllers, the relative power is measured as a function of the polarizer angle. The measurement is conducted at thirty minutes intervals after starting fiber laser operation and after one restart. The result shows that the polarization of the fiber laser remains stable for an extended period of time and after a restart.

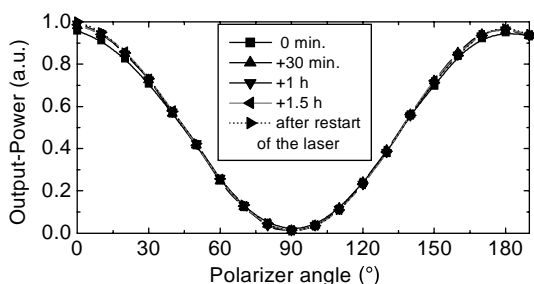


Fig. 2. Polarization stability evaluation of the fiber laser. This figure indicates that the polarization is stable for 1.5 hours and after a restart.

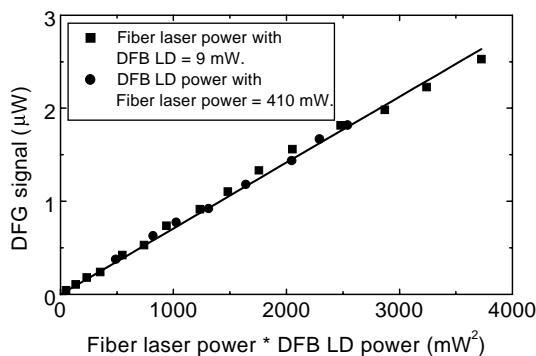


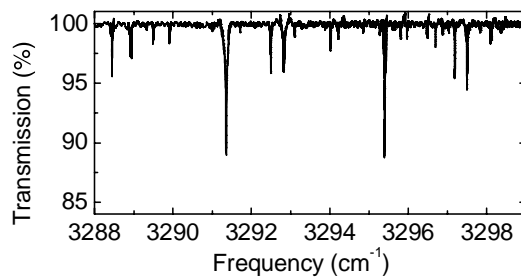
Fig. 3. DFG power at $3\ \mu\text{m}$ as a function of the incident pump power product of a fiber laser and a DFB LD using a 20.5 mm long PPLN crystal. Solid squares are used for varying fiber laser power with fixed DFB LD power of 9 mW while solid circles are used to indicate varying DFB LD power with fixed fiber laser power of 410 mW. The slope efficiency is estimated to be $0.72\ \text{mW/W}^2$.

3.1 DFG slope efficiency

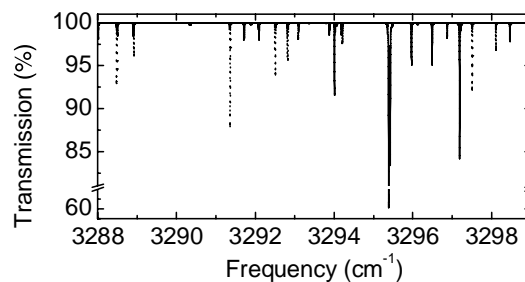
Figure 3 depicts the DFG power output as a function of the product of incident pump powers from both fiber and the DFB diode lasers. The pump powers used are the values at the entry facet of the PPLN crystal. First the fiber laser power is varied with constant DFB LD power of 9 mW (solid square dots) and subsequently the DFB LD power is varied with constant fiber laser power of 410 mW (solid circle dots). The DFG slope efficiency is estimated to be $0.72\ \text{mW/W}^2$ ($0.36\ \text{mW/W}^2$ per 1 cm crystal length). The DFG power of $2.5\ \mu\text{W}$ from this source is obtained for a product of $\sim 3700\ \text{mW}^2$ when the fiber laser power is 410 mW and DFB LD power is 9 mW. The theoretically calculated slope efficiency¹⁾ using an effective nonlinear coefficient $d_{\text{eff}} = 14\ \text{pm/V}$, a confocal parameter $b = 0.17$ and focusing function $h = 0.35$ can be estimated to be $\sim 1.5\ \text{mW/W}^2$ for our experimental condition. The discrepancy between theoretical estimation and experimental result is most likely due to such factors as absorption losses in the optical components and crystal, and non-perfect phase matching by the PPLN. However, the result is in good agreement with the previous experimental work such as in ref. 24.

3.2 Spectroscopic performance

Figure 4(a) shows the NH_3 and H_2O (due to impurities) spectrum at $\sim 3294\ \text{cm}^{-1}$ obtained by frequency-scanning the DFG spectroscopic source at a cell pressure of 400 Pa. The frequency tuning range of the DFG spectroscopic source is demonstrated to be $>10\ \text{cm}^{-1}$ (300 GHz). The figure depicts continuously tunable operation without any frequency mode



(a)



(b)

Fig. 4. (a) Experimental NH_3 spectrum at $\sim 3294\ \text{cm}^{-1}$ at a cell pressure of 400 Pa and a path length of 10.2 cm. A frequency tuning range of $10\ \text{cm}^{-1}$ (300 GHz) is obtained. (b) Simulated NH_3 spectrum at $\sim 3294\ \text{cm}^{-1}$ from HITRAN96 database. The solid line shows the NH_3 absorption lines at a pressure of 400 Pa while H_2O absorption lines are shown as a dotted lines assuming a pressure of 930 Pa. The path length is 10.2 cm.

hop. Figure 4(b) shows the expected spectrum at $\sim 3294\ \text{cm}^{-1}$ obtained from the HITRAN96 database.²⁵⁾ The solid lines shows NH_3 absorption lines at the same condition as used in the experiment. The H_2O absorption lines are depicted as dotted lines assuming a pressure of 930 Pa.

A high-resolution Doppler-broadened NH_3 absorption spectrum around at $3295.4\ \text{cm}^{-1}$ ($3.0345\ \mu\text{m}$) at a cell pressure of 27 Pa is obtained as shown with an upper trace in Fig. 5. The two lines are identified as absorption lines at $3295.388\ \text{cm}^{-1}$ (absorption strength = $7.99 \times 10^{-21}\ \text{cm/molecule}$) and $3295.426\ \text{cm}^{-1}$ (absorption strength = $3.05 \times 10^{-21}\ \text{cm/molecule}$) respectively, separated by $0.0375\ \text{cm}^{-1}$ belonging to the ν_1 band at $3\ \mu\text{m}$.

The spectrum is fitted by a Gaussian profile. The linewidth of the absorption lines is measured to be $0.011\ \text{cm}^{-1}$ (330 MHz) (FWHM) and $0.010\ \text{cm}^{-1}$ (300 MHz), respectively. Values obtained from the HITRAN96 database ($0.011\ \text{cm}^{-1}$ (330 MHz))²⁶⁾ agree within $0.001\ \text{cm}^{-1}$ (30 MHz). This measurement demonstrates that the spectral resolution of the DFG source is less than $0.001\ \text{cm}^{-1}$.

The fit residual is obtained by subtracting the fit profile from the data as shown with a lower trace in Fig. 5. The residual is found to be within 0.15%, which corresponds to an absorption sensitivity of 6.6×10^{-4} at a frequency of $3295.388\ \text{cm}^{-1}$. This residual is due to a combination of factors, such as optical noise in each pump source and optical interference effects. Another absorption line at $3295.426\ \text{cm}^{-1}$ exhibits better fit value as low as 0.04% probably due to interference free from H_2O absorption. A 40 ppm-m (parts per million per meter) NH_3 detection limit can be estimated in the

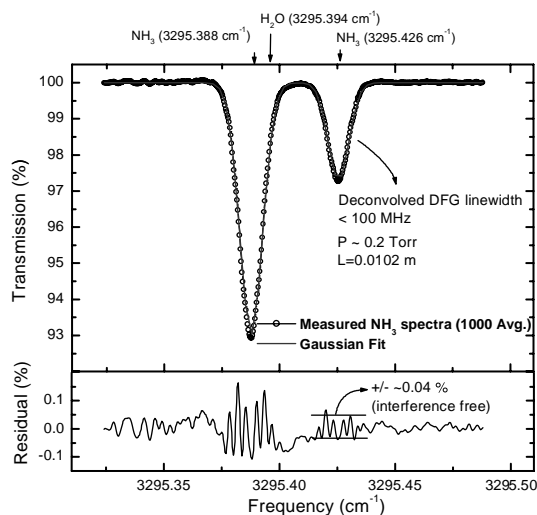


Fig. 5. Upper trace shows high-resolution NH_3 absorption Doppler-broadened spectrum at 3295.4 cm^{-1} ($3.0345\text{ }\mu\text{m}$) at a cell pressure of 27 Pa and a path length of 10.2 cm. This measurement is made with 1000 scan averages at a 370 Hz modulation frequency. Lower trace is the fit residual by subtracting the Gaussian lineshape from the measured absorption.

pressure broadened regime (greater than 30 kPa).

4. Conclusions

A DFG based narrow-linewidth spectroscopic source pumped by high power fiber laser and DFB laser diode combination is demonstrated successfully at $3\text{ }\mu\text{m}$. A mid-IR power of $\sim 2.5\text{ }\mu\text{W}$, a spectral linewidth of $< 30\text{ MHz}$ and frequency tunability of $> 300\text{ GHz}$ are obtained. A high resolution Doppler-broadened NH_3 spectrum of 3295.4 cm^{-1} is detected with a 10.2-cm-long gas cell at a pressure of 27 Pa, from which we can estimate a detection limit as 24 ppm-m at pressures in the Lorentzian-broadened pressure region ($> 30\text{ kPa}$). This first demonstration is helpful in the design of DFG based gas sensors utilizing present and future advances in optical fiber and photonic technologies.

- 1) P. Canarelli, Z. Benko, R. F. Curl and F. K. Tittel: *J. Opt. Soc. Am. B* **9** (1992) 197.
- 2) L. Goldberg, W. K. Burns and R. W. McElhanon: *Appl. Phys. Lett.* **67** (1995) 2910.
- 3) A. Balakrishnan, S. Sanders, D. DeMars, J. Webjorn, D. W. Nam, R. J. Lang, D. G. Mehuys, R. G. Waarts and D. F. Welch: *Opt. Lett.* **21** (1996) 952.
- 4) D. G. Lancaster, L. Goldberg, J. Koplów, R. F. Curl and F. K. Tittel: *Electron. Lett.* **34** (1998) 1345.
- 5) D. Mazzotti, P. De Natale, G. Giusfredi, C. Fort, J. A. Mitchell and L. W. Hollberg: *Appl. Phys. B* **70** (2000) 747.
- 6) D. Richter, D. G. Lancaster and F. K. Tittel: *Appl. Opt.* **39** (2000) 4444.
- 7) M. M. Fejer, G. A. Magel, D. H. Jundt and R. L. Byer: *IEEE J. Quantum Electron.* **28** (1992) 2631.
- 8) D. G. Lancaster, R. Weidner, D. Richter, F. K. Tittel and J. Limpert: *Opt. Commun.* **175** (2000) 461.
- 9) Y. Mine, N. Melander, D. Richter, D. G. Lancaster, K. P. Petrov, R. F. Curl and F. K. Tittel: *Appl. Phys. B* **65** (1997) 771.
- 10) K. P. Petrov, L. Goldberg, W. K. Burns, R. F. Curl and F. K. Tittel: *Opt. Lett.* **21** (1996) 86.
- 11) M. Feher and P. A. Martin: *Spectrochim. Acta Pt. A* **51** (1995) 1579.
- 12) F. Capasso, C. Gmachl, A. Tredicucci, A. L. Hutchinson, D. L. Sivco and A. Y. Cho: *Opt. & Photon. News* **10** (1999) No. 10, 31.
- 13) A. J. Henderson, P. M. Roper, L. A. Borshowa and R. D. Mead: *Opt. Lett.* **25** (2000) 1264.
- 14) D. Hofmann, G. Schreiber, C. Haase, H. Herrmann, W. Grundkotter, R. Ricken and W. Sohler: *Opt. Lett.* **24** (1999) 896.
- 15) K. P. Petrov, A. P. Roth, T. L. Patterson, T. P. S. Thoms, L. Huang, A. T. Ryan and D. J. Bamford: *Appl. Phys. B* **70** (2000) 777.
- 16) N. Saito, S. Wada, H. Taniguchi, M. Nakamura, Y. Urata and H. Tashiro: *Jpn. J. Appl. Phys.* **39** (2000) 1767.
- 17) K. Frandkin-Kashi, A. Arie, P. Urenski and R. Rosenman: *Appl. Phys. B* **71** (2000) 251.
- 18) H. Parhat, N. J. Vasa, T. Okada, M. Maeda and H. Taniguchi: *Jpn. J. Appl. Phys.* **39** (2000) L800.
- 19) H. M. Pask, R. J. Carman, D. C. Hanna, A. C. Tropper, C. J. Mackechnie, P. R. Barber and J. M. Dawes: *IEEE J. Sel. Top. Quantum Electron.* **1** (1995) 2.
- 20) L. Goldberg, J. P. Koplów and D. A. V. Kliner: *Opt. Lett.* **24** (1999) 673.
- 21) K. P. Petrov, R. F. Curl, F. K. Tittel and L. Goldberg: *Opt. Lett.* **21** (1996) 1451.
- 22) L. E. Myers, R. C. Eckardt, M. M. Fejer and R. L. Byer: *J. Opt. Soc. Am. B* **12** (1995) 2102.
- 23) D. H. Jundt: *Opt. Lett.* **22** (1997) 1553.
- 24) D. G. Lancaster, D. Richter, R. F. Curl, F. K. Tittel, L. Goldberg and J. Koplów: *Opt. Lett.* **24** (1999) 1744.
- 25) HITRAN96, Ontar Corporation, North Andover, MA, USA.